SNOTEL REPRESENTATIVENESS IN THE RIO GRANDE HEADWATERS ON THE BASIS OF PHYSIOGRAPHICS AND REMOTELY-SENSED SNOW COVER PERSISTENCE

Noah P. Molotch[1] and Roger C. Bales[2]

ABSTRACT

Snowpack telemetry (SNOTEL) sites in and around the Rio Grande headwaters basin are located at the middle elevations of the watershed, in relatively dense vegetation, and toward the western boundary of the watershed. Based on 8 years of Advanced Very High Resolution Radiometer data (1995 – 2002), the snow cover persistence index value at the six SNOTEL sites ranged from 3.9 to 4.4 with an average 12% greater than the mean persistence of the watershed. Therefore, information from the sites does not capture the variability in snowpack accumulation and ablation processes across the watershed. Using elevation, western barrier distance, and vegetation density, a 32-node binary regression tree model explained 75% of the variability in average snow-cover persistence. Terrain classes encompassing the Lily Pond, Middle Creek, and Slumgullion SNOTEL sites represented 4.1, 6.4, and 4.0% of the watershed area, respectively. SNOTEL stations do not exist in the spatially extensive (e.g. 11% of the watershed) terrain classes located in the upper elevations above timberline. The results and techniques presented here will be useful for spatially distributed hydrologic analyses in that we have identified the physiographic conditions currently represented by SNOTEL stations (i.e. the snowpack regimes at which SWE estimation uncertainty can be determined). Further, we have outlined a statistically unbiased approach for designing future observation networks based on variability in physiographic attributes and snowpack processes.

INTRODUCTION

The most widely-used ground-based observations for evaluating, initializing, and updating grid element snowpack estimates currently come from the snowpack telemetry (SNOTEL) network. The intended purpose of the SNOTEL network is to replace the snow courses that provide information for runoff volume forecasting using empirical relationships between point values of SWE, antecedent soil moisture, historical temperature and precipitation data and observed runoff. Relying on these empirical techniques in coming decades could be problematic given that these techniques perform poorly for conditions not well represented in the historical record (T. Pagano, Natural Resource Conservation Service (NRCS), personal communication, 2004). Such conditions are likely given observed and projected changes in snowpack processes (National Research Council, 2005).

Snow courses (and SNOTEL) were placed in areas that are representative of the water producing regions of a watershed (U.S. Soil Conservation Service, 1972). The snow courses were installed in the 1930's with the main criteria being site accessibility and protection from public disturbance (Mike Gillespie, NRCS, personal communication, 2004). Though the manual snow courses provide many long time series, and the snow telemetry stations provide daily or even hourly temporal resolution, their locations may not represent the full range of physiographic conditions found within the watersheds in which they are located. Such observations are needed to develop a physical understanding of the processes that control snow distribution and snowmelt. Furthermore, these observations are needed to evaluate spatially distributed hydrologic model performance as physiographics can control algorithm performance in non-linear ways (Beven, 1995).

Identifying the continuum of SWE variability and the physiographic controls on that variability is difficult over larger watersheds (e.g. > 1000 km^2) as remotely sensed SWE data are not available at sufficiently fine resolutions (i.e. < 25 km^2). Similarly, the spatial variability in snow distribution at these scales cannot be resolved using current ground observations as the distance between observations is greater than the correlation length scale (Blöschl, 1999). Analyses of the physiographic controls on snow cover persistence may be useful for classifying zones of snow cover processes as snow cover persistence varies as a function of both snow accumulation and snowmelt processes.

Paper presented Western Snow Conference 2005
[1] Cooperative Institute for Research in Environmental Sciences, University of Colorado, Boulder, CO. 80309, USA
[2] Division of Engineering, University of California, Merced, CA, 95344, USA

Statistically significant relationships between snow accumulation and physiographic variables exist at the hill-slope scale (Elder, et al., 1998; Molotch, et al., 2005) and at the regional scale (Fassnacht, et al., 2003; Molotch, et al., 2004b; Solomon, et al., 1968). Regression tree snow depth models have been used to explore these relationships at the hill-slope scale (Balk and Elder, 2000; Elder, et al., 1995; 1998; Erxleben, et al., 2002; Molotch, et al., 2005; Winstral, et al., 2002) but have not been used at larger scales (i.e. > 1000 km^2) due to the small spatial density of ground observations at these scales.

Physiographics also control the spatial patterns of snow ablation as vegetation and topography influence the distribution of solar radiation (Davis, et al., 1997; Dozier, 1980), snow-surface albedo (Molotch, et al., 2004a), net longwave radiation (Sicart, *et al.*, 2004), wind speed, and turbulent fluxes (Cline and Carroll, 1999).

In this research binary regression tree models are used to relate physiographics (i.e. independent variables) to remotely sensed snow cover persistence (i.e. dependent variable). These relationships are then used to identify the representativeness of SNOTEL and the optimal locations for future observations. Three questions are addressed. First, what are the physiographic conditions currently represented at the SNOTEL sites relative to the watershed? Second, how persistent is snow cover at the SNOTEL sites relative to the persistence of snow across the watershed? Finally, what are the relationships between physiographics and snow cover persistence across the watershed and how do these relationships control SNOTEL representativeness?

STUDY AREA

This study was conducted in an area surrounding the Rio Grande headwaters in the San Juan Mountains of southern Colorado (Figure 1a). The Rio Grande headwaters basin encompasses an area of 3,419 km^2, with a minimum elevation of 2,434 m at the U.S. Geological Survey (USGS) Del Norte streamflow gauge and a maximum elevation of 4,233 m. Approximately 50% of the watershed is covered with coniferous forests. Herbaceous grasslands of the valley floor and alpine zones cover approximately 35% of the watershed, with the remaining 15% mixed between deciduous forests, shrublands and bare ground. The watershed is surrounded by the continental divide on its western, northern and southern boundaries, separating it from the San Juan and Gunnison River basins to the southwest and north, respectively. Draining to the east, runoff from the basin provides the primary source of surface water for the highly productive agricultural lands in the San Luis Valley and for meeting the water allocation requirements to the down-river States under the Rio Grande Compact. Precipitation in the San Luis Valley is less than 25 cm on average, but a substantial aquifer provides storage of snowmelt-derived recharge from the Sangre de Cristo and San Juan Mountains.

Mean SWE for the period of record for each site is shown in Figure 1b. Metadata associated with the six SNOTEL stations studied here are outlined in Table 1.

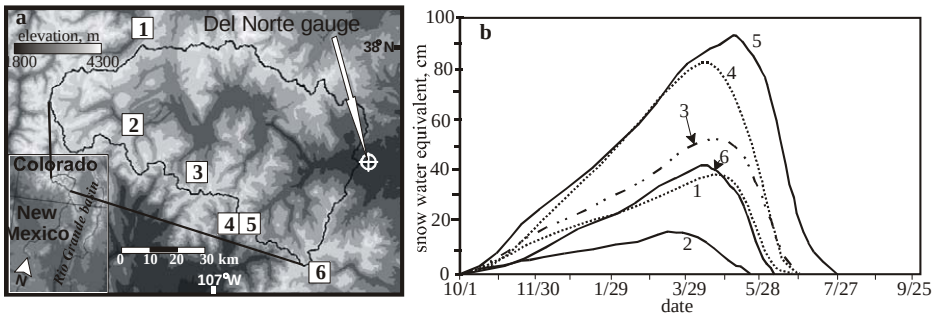

Figure 1. (a) The Rio Grande above Del Norte and the Slumgullion (1), Upper Rio Grande (2), Middle Creek (3), Upper San Juan (4), Wolf Creek (5), and Lily Pond (6) SNOTEL sites. (b) Average SNOTEL snow water equivalent, water years 1981 – 2000. Sites are numbered 1 – 6 corresponding to (a).

Table 1. Attributes of the six SNOTEL in the Rio Grande headwaters used in the analysis.

site	[a]forest density, %	[b]elevation, m	[c]installed	[d]maximum SWE, cm
Slumgullion	82	3581	1980	42
Upper Rio Grande	62	2855	1987	17
Middle Creek	40	3430	1980	53
Upper San Juan	71	3089	1979	83
Wolf Creek Summit	76	3331	1987	94
Lily Pond	68	3374	1980	43

data source: [a] USGS EROS data center, [b,c,d] NRCS National Water and Climate Center. [d]Values are average annual maximum SWE from installation year to 2002.

STUDY PERIOD

During the period 1995 – 2002 measured maximum SWE accumulation at the six SNOTEL sites ranged from 38% of average in 2002 to 139% of average in 1997 (Figure 2). Significant variability existed between SNOTEL sites during some water years; e.g. in 2002 maximum SWE at Lily Pond was 102% of normal while Upper Rio Grande was 160% of normal (Figure 2). In 1998 the percent of mean values at the SNOTEL sites ranged by only 11% (Figure 2). The range of percent of mean values during the period 1995 – 2002 averaged 37%.

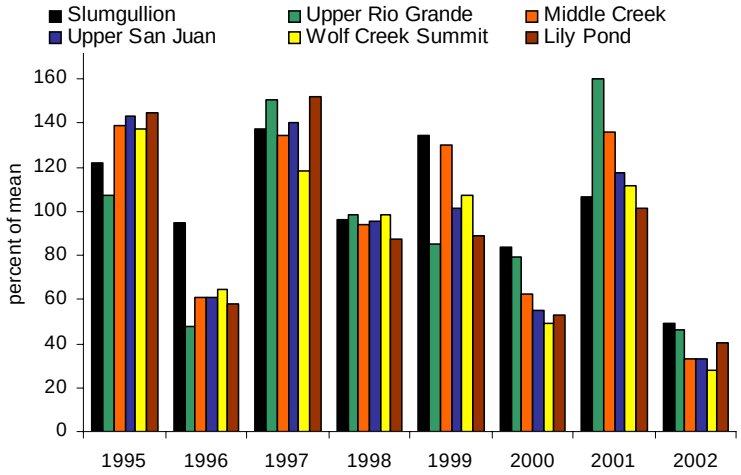

Figure 2. The maximum snow water equivalent measured at the six SNOTEL sites 1995 – 2002. Values shown are the percentage of the mean maximum SWE over the period of record. Sites 1 – 6 (using the numbering scheme from Figure 1) are shown from left to right for each year.

METHODS

Physiographic Variables

Using a geographical information system (GIS), the topographic variables elevation, slope and aspect were obtained from the level 1 standard 7.5-minute, 30-m resolution, U.S. Geological Survey, Digital Elevation Model (DEM).

The solar radiation index was calculated assuming clear-sky conditions using the TOPQUAD algorithm (*Dozier*, 1980). Daily-integrated net solar radiation was calculated for each 30-m pixel within the study area on the

15th of each month for the 2001 snow accumulation and snowmelt season (i.e. November 2000 – June 2001). The solar radiation index was obtained by summing the daily-integrated surfaces from November 15th to the 15th of the respective month at which snow cover persistence was calculated. Given that the solar radiation is a clear-sky index its use was assumed transferable to other water years.

The mean maximum upwind slope, Sx, is a terrain-based parameter designed to capture the variability in snow deposition as a result of wind redistribution (Winstral, et al., 2002). The availability of wind speed data in the higher elevations of the Rio Grande is limited. Data from the Colorado Agricultural Research Station at Center, Colorado from November – April, water years 2001 and 2002 were used to identify conditions conducive to redistribution of snow by wind. These two water years were chosen given data availability and the high variability between the two water years (Figure 2). Relative frequency histograms of wind speed, wind direction, and relative humidity were used to define the wind direction of events most likely to redistribute snow (Figure 3). Redeposition of snow by wind is most likely to occur during and immediately after snowfall and when wind speeds are high. Relative humidity data were included as an indication of snowfall. A 60° pie-shaped area centered on the upwind direction (Figure 3) with a radius of 100 m was used to define the upwind area of each 30-m source pixel (Molotch, et al., 2005; Winstral, et al., 2002). The maximum upwind slope was then calculated for each 30-m cell following the methods of Winstral et al. (2002). Maximum upwind slope as well as all other 30-m resolution variables were resampled to 1-km to match the resolution of the AVHRR data.

Vegetation density has been shown to play a role in snow distribution by altering the energy balance at the snow/atmosphere interface, intercepting snowfall and by influencing the surface roughness and the wind fields that transport snow (Gray and Male, 1981). Vegetation density data at 1-km resolution were derived from AVHRR data obtained from the USGS EROS Data Center, Global Land Cover Characterization data set (http://edc.usgs.gov/products/landcover/glcc.html).

The western barrier distance, *bar_d*, is a measure of the distance between each 1-km^2 cell within the study region and the highest point between that cell and a significant moisture source (Fassnacht, et al., 2001). In this research the moisture source was considered to be the Pacific Ocean and therefore *bar_d* was determined as the distance to the highest point between the source cell and the Pacific Ocean along a vector of 270° from north.

The physiographic conditions at the SNOTEL sites were compared to the basin-wide statistical distribution of the physiographic variables described above.

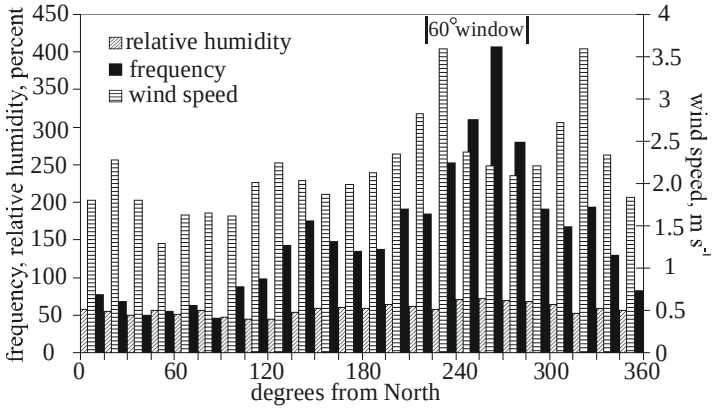

Figure 3. Histogram of wind direction measured at the Center, Colorado Co-agmet meteorological station from 9 November 2001 to 10 April 2002 with the 60° window used to define the upwind area from each source cell in the calculation of the maximum upwind slope, Sx (degrees). Sx is a terrain-based parameter designed to represent the variability in snow deposition as a result of wind redistribution.

Snow Cover Persistence

Assessing the representativeness of SNOTEL SWE observations relative to the SWE distribution of the Rio Grande headwaters is not realistic because obtaining ground-truth estimates of SWE over large areas (i.e. 3,419 km^2) is logistically prohibitive. Therefore, for the purposes of assessing the representativeness of the snowpack characteristics measured at SNOTEL sites relative to the watershed, SCA persistence maps were derived. This

approach is valid given that patterns of snow cover depletion vary as a function of both snow accumulation and snowmelt processes. Recent advancements in ability to detect snow covered area from the Moderate Resolution Imaging Spectroradiometer (MODIS) (Klein and Stroeve, 2002) drive the need to study snowpack processes using time-series of these data. MODIS data are not yet available over the period of record analyzed under this research but our use of AVHRR data is intended to show proof of concept for future use of other remotely sensed snow cover products as their record length becomes sufficient.

Fractional SCA data were generated with a spectral mixture analysis (Rosenthal, 1996) of Advanced Very High Resolution Radiometer (AVHRR) imagery for cloud-free acquisitions from 1995 – 2002 (Bales, et al., 2003). The fractional SCA grids were resampled to binary SCA based on the condition that any detectable amount of SCA (SCA > 0%) is a snow-covered pixel and assigned a value of 1, with all other cloud-free pixels assigned a value of 0 (*Molotch, et al.*, 2004b). Snow cover persistence maps were then derived for the months of April, May and June, where a value of 1 – 8 assigned to each 1-km^2 pixel based on the number of years during the period 1995 – 2002 where snow cover was detected during a given month. Additionally, an average snow cover persistence map was calculated as the mean number of months (January – June) with observed snow cover during any acquisition date within a given month for the years 1995 – 2002.

Clouds often contain similar reflective and brightness temperature characteristics to those of snow. Cloud masks were generated by an image analysis (Simpson, et al., 1998) to eliminate those pixels determined to be clouds rather than snow. This technique required manual interpretation and editing of pixels. Water and highly reflective land features were also manually masked to prevent interpretation as snow.

Fractional SCA estimates from the Landsat 7 Enhanced Thematic Mapper (TM) acquired on 1 April 2001, 17 April 2001, 19 March 2002, and 4 April 2002 were used to estimate the accuracy of the AVHRR SCA estimates. Additional TM acquisitions were not used in the error analysis due to the presence of cloud-cover and budgetary constraints. The accuracy assessment from 2001 and 2002 - two dramatically different (Figure 2) water years - are assumed to be transferable to the other water years of this study. Fractional snow covered area (SCA) estimates from TM data were derived using the spectral mixture analysis algorithm of Painter et al. (2003). Cloud-masks for the TM data were not necessary as selected scenes were cloud-free. The 30-m TM data were resampled to 1-km in order to match the resolution of the AVHRR data.

Erroneously omitted pixels were determined as those in which AVHRR detected no snow whereas TM detected snow (Cline and Carroll, 1999). Erroneously committed pixels were determined as those in which AVHRR detected snow whereas TM did not. Omission errors were summarized as the percentage of snow covered pixels erroneously omitted. Conversely, committed errors were summarized as the percentage of snow-free pixels erroneously committed.

Binary Regression Trees

Binary regression tree models classify dependent variables from a suite of independent variables in a non-linear hierarchical fashion. These models have been successfully used to predict snow cover persistence at the hill-slope scale (Anderton, *et al.*, 2004). The use of these models to identify zones of snowpack processes (i.e. snow accumulation and snowmelt processes) is necessary as snowpack processes are often related to independent variables in a non-linear fashion. Increasingly homogeneous subsets of average snow cover persistence (i.e. the dependent variable) were binned using binary recursive partitioning. Various combinations of the aforementioned independent variables were included into separate tree models (Molotch, et al., 2005). For each of these combinations a classification tree was intentionally grown to over-fit the data as described in Chambers and Hastie (1993). The mean model deviance from one hundred iterations of ten-fold cross-validation procedures were plotted as a function of the number of terminal nodes (Molotch, et al., 2005). Tree sizes that minimized model deviance were examined for further consideration. The coefficient of determination, R^2, for classification trees ranging from 2 to 40 terminal nodes were plotted versus number of terminal nodes. Tree models that minimized deviance and maximized model fit (i.e. R^2) were selected as the best models. The model resulting in the minimum deviance was used to classify zones of average snow cover persistence across the watershed. The percent of watershed area represented by each class was used to identify optimal areas for future observations and to determine the percentage of watershed area represented by the current SNOTEL observation network. A detailed description of the tree fitting, pruning and cross-validation procedures can be found in Breiman et al. (1984), and applications to snow hydrology are given in Elder *et al.* (1995; 1998).

Optimal areas for observing snowpack processes are those that represent a significant portion of the watershed. However, the ability of a point observation to represent the encompassing terrain class (i.e. terminal node) is largely dependent upon the deviance in snow cover persistence within the class. Hence, identification of SNOTEL representativeness and the optimal areas for future observations were further evaluated by examining the ratio between the areal extent of a given terrain class and the deviance of snow cover persistence within the respective terrain class.

RESULTS

Physiographic Variables

Due to the topographic complexity of the watershed the spatial distribution of the solar radiation index was highly variable, ranging from 151 to 303 W m^{-2}. Vegetation density was greatest toward the southern boundary of the watershed with a basin-wide mean of 53% and coefficient of variation of 0.38. The spatial distribution of maximum upwind slope, *Sx*, exhibited a relatively repeating structure with prominent ridges – which divide negative *Sx* values from positive values – organized in a north / south orientation. Intuitively, the *western barrier distance* decreased toward the western end of the watershed. Decreases in *western barrier distance* were also apparent in the southeastern portions of the watershed due to the northwestern / southeastern orientation of the southern watershed boundary. The mean *western barrier distance* was 48 km with a coefficient of variation of 0.6. Given that the *western barrier distance* approached 0 at the western edges of the watershed it can be concluded that the largest barrier between grid-cells within the watershed and the Pacific Ocean are the immediate watershed divides as apposed to mountain ranges outside the basin to the west.

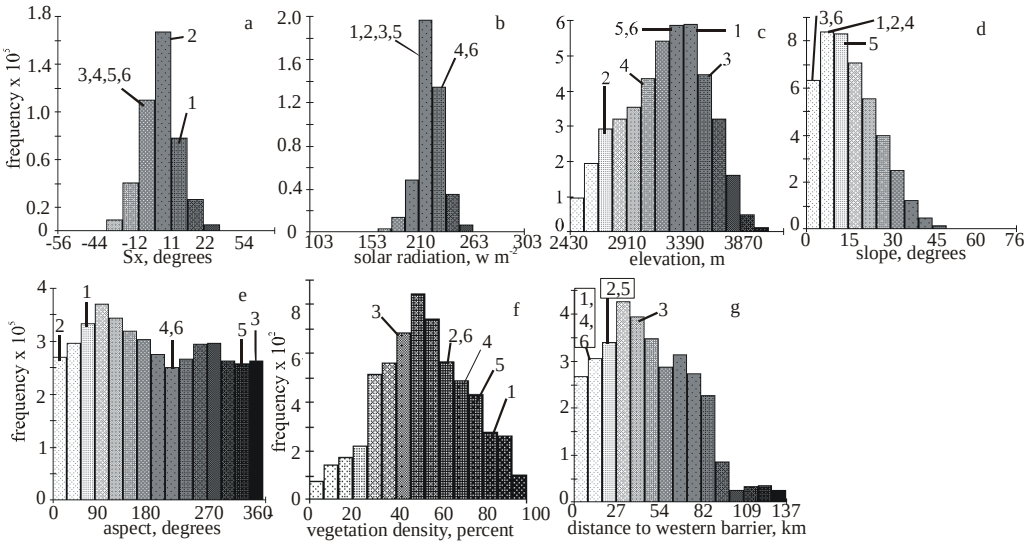

Figure 4. The statistical distribution of physiographic variables that potentially influence snow distribution. (a) The maximum upwind slope, Sx, is a terrain-based parameter designed to represent the variability in snow deposition as a result of wind redistribution. (b) The solar radiation index is a summation of the daily-integrated modeled solar radiation from November 15th to April 15th. Elevation (c), slope (d), and aspect (e) were derived from the standard USGS 30-m digital elevation model. (f) Vegetation density was obtained from the USGS EROS Data Center, Global Land Cover Characterization data set. (g) Western barrier distance is an index intended to account for orographics and was computed as the distance to the highest point between each source cell and potential moisture sources to the west.

The SNOTEL sites in and around the Rio Grande headwaters basin are not located in areas that are representative of the physiographic conditions of the watershed (Figure 4a-g). Stations are located at the middle to lower elevations of the watershed (Figure 4c), in densely forested areas (Figure 4f), on north- and south-facing slopes (Figure 4e), on flatter slopes (Figure 4d), and close to the western barrier (Figure 4g).

Snow Cover Persistence

Intuitively, snow cover persistence decreased toward the lower elevations of the watershed (Figure 5a-c). Snow cover persisted into the month of April at every grid-cell in the watershed in at least 1 of the years 1995 – 2002 (Figure 5a). The mean value of the average snow cover persistence map (not shown) was 3.7 with a standard deviation of 0.07.

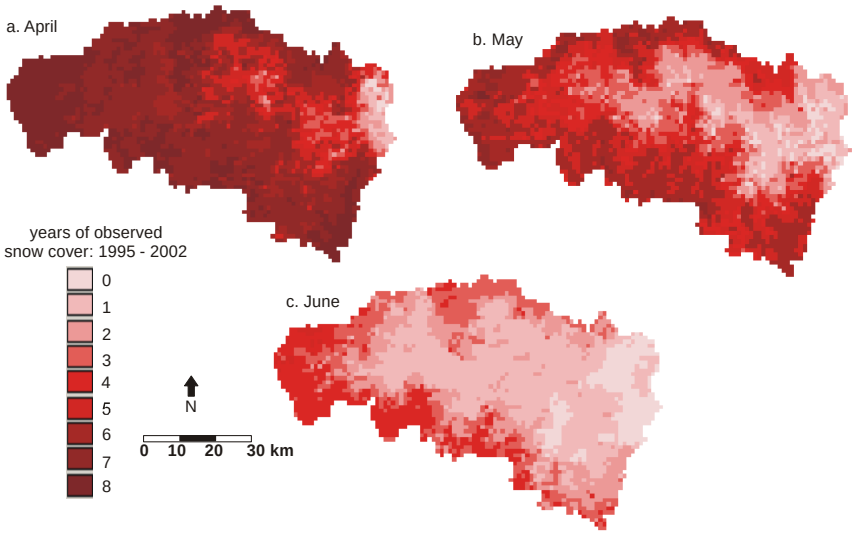

Figure 5. The spatial distribution of snow cover persistence for April (a), May (b) and June (c), 1995 – 2002. Values are the number of years during the 8-year period in which snow cover was observed by AVHRR during the respective month.

SNOTEL stations are located in areas with relatively persistent May and June snow cover (Figure 6a,b). Average snow cover persistence values at the SNOTEL sites ranged from 3.875 at Lily Pond to 4.375 at Slumgullion and Upper San Juan. The mean value of the average snow cover persistence at the 6 SNOTEL sites was 4.125 or 12% greater than the watershed mean. The statistical distribution of snow cover persistence is skewed toward more persistent snow cover at shorter distances to the western barrier and toward less persistent snow cover at longer distances (Figure 7a,b). The shift in skew from more persistent to less persistent snow cover occurred at a relatively short distance to the western barrier (i.e. 48 km) for the May persistence map (Figure 7a). The shift in skew occurred at a shorter distance (i.e. 19 km) for the June persistence map (Figure 7b). With locations toward the western barrier (Figure 4g) and therefore in areas with greater snow cover persistence, SNOTEL stations are located in the "water producing" regions of the watershed – as they were intended – and not in areas that capture the variability in snow characteristics across the watershed.

Figure 6. Histograms of snow cover persistence for May (a) and June (b), 1995 – 2002. Abscissa bins are the number of years during the 8-year period in which snow cover was observed by AVHRR. Values indicated on each panel correspond to the SNOTEL sites listed in Figure 1. Note: Wolf Creek Summit was likely in abscissa bin 5 as georegistration issues may have caused misclassification.

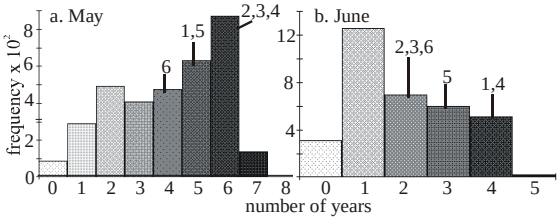

The AVHRR SCA estimates underestimated snow covered areas in the lower elevations of the watershed and hence omission errors were 1.9 times greater than commission errors on average (Table 2). These omission errors seem to be more prominent south of the valley floor which is likely due to the combined effect of terrain illumination and vegetation density – both of which can increase omission errors (Rosenthal, 1996). A detailed assessment of the controls on SCA algorithm accuracy is beyond the scope of this research. Average map accuracies were 62% for the 4 image comparisons. Map accuracies were greatest at time periods when snow cover was relatively continuous. Given the relatively low commission errors, snow cover persistence estimates were considered conservative in that snow cover persisted at least as long as it was detectable from AVHRR data.

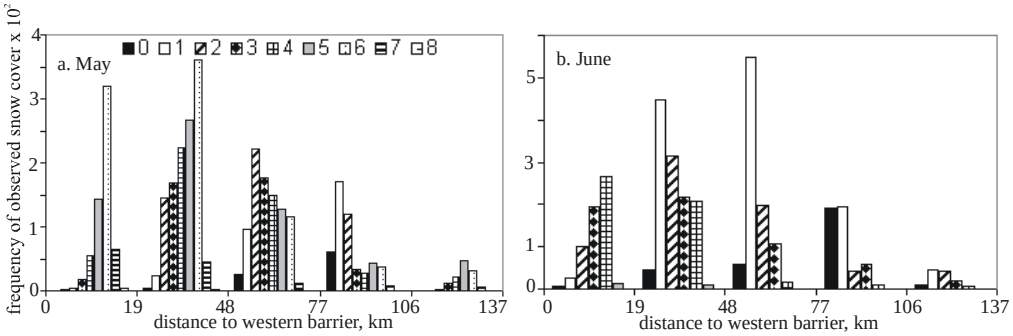

Figure 7. May (a) and June (b) snow cover persistence (for the same 8-year period as Figure 6 at different distances from the western boundary. Histograms for shorter distances are skewed toward more persistent snow cover – larger distances toward less persistent snow cover.

Table 2. Error statistics and map accuracies for four AVHRR snow covered area images with Landsat 7 ETM+ data used to estimate errors.

	1 April 2001	17 April 2001	19 March 2002	4 April 2002
comission error, %	29.9	13.5	1.1	1.3
omission error, %	12.2	25.4	51.7	17.3
map accuracy, %	58.0	61.1	47.2	81.4

Binary Regression Trees

The cross-validation showed that model deviance was minimized using the solar radiation index, elevation, *western barrier distance* and vegetation density in the model development (Figure 8a). Deviance was minimized using a 32 terminal-node classification tree. Minimum model deviance increased substantially with the exclusion of western barrier distance (Figure 8a). Slight increases in minimum deviance resulted from the inclusion of slope, aspect and maximum upwind slope (Figure 8a). Model fit improved notably with the inclusion of *western barrier distance* (Figure 8b).

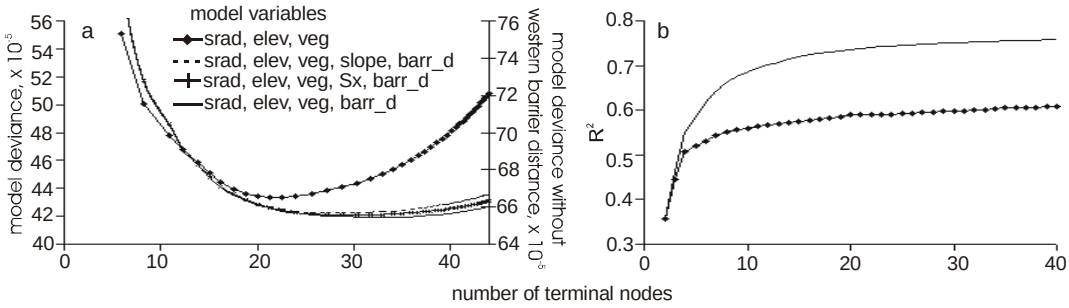

Figure 8. Model deviance (a) and coefficient of determination (R^2) (b) versus number of terminal nodes for regression tree models developed elevation (*elev*), the solar radiation index (*srad*), vegetation density (*veg*), maximum upwind slope (*Sx*), slope, aspect, and western barrier distance (*bar_d*). All models included elevation, solar radiation, and vegetation density.

Using elevation, western barrier distance, and vegetation density the 32-node tree model explained 75% of the variability in snow-cover persistence – a considerable improvement over the explanatory ability of either elevation (66%) or western barrier distance (50%). Although these two independent variables were significantly correlated ($R^2 = 0.15$, $p = 0$), the control of western barrier distance on snow cover persistence was considerable as indicated by the frequent appearance of the variable at upper tree model levels (Figure 9) (Elder, 1995). Intuitively, snow cover persistence increased with elevation and decreased with distance to the western barrier.

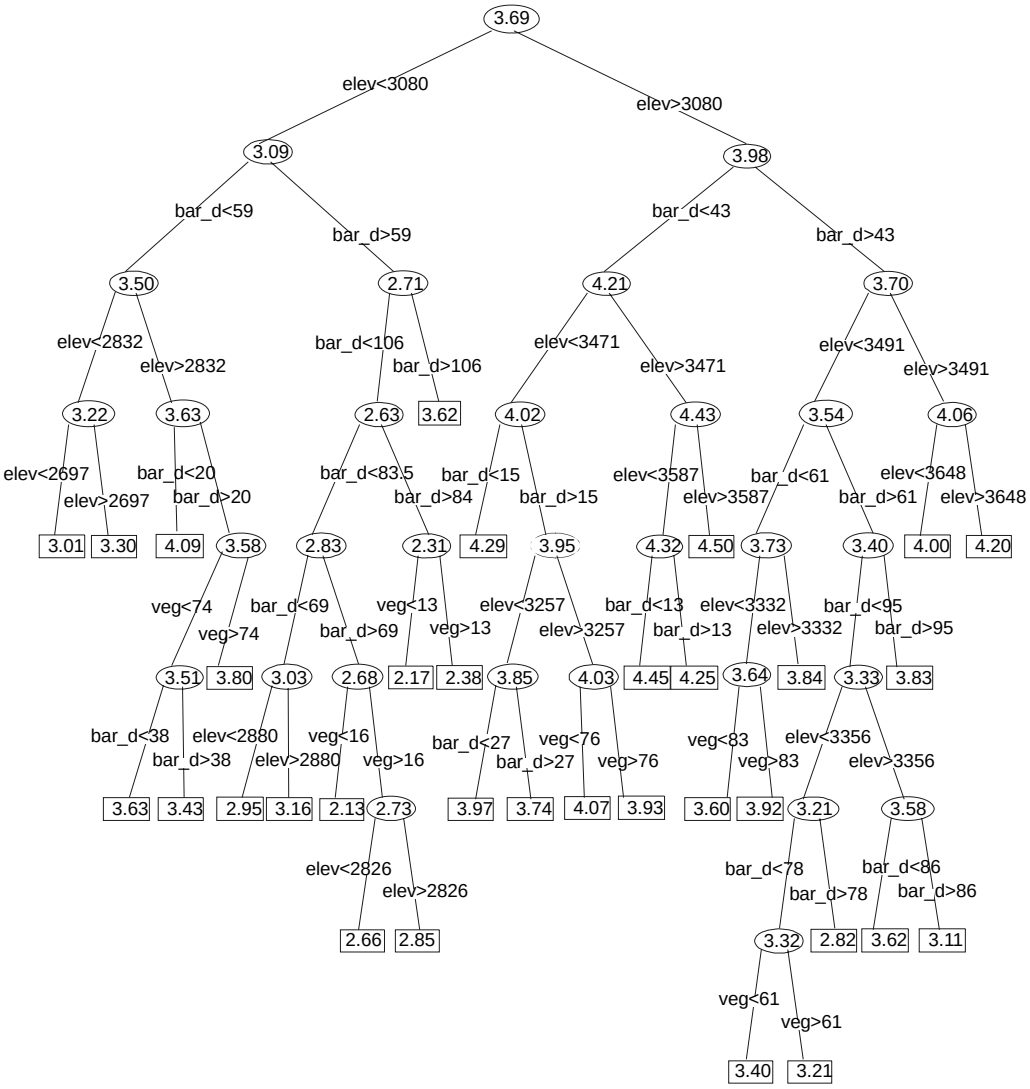

Figure 9. Thirty two termnal-node binary regression tree model relating independent variables of elevation (*elev*), western barrier distance (*bar_d*), and vegetation density (*veg*) to the dependent variable average snow cover persistence (decimal months) over the period 1995 – 2002. Units for the 3 independent variables are m, km, and percent, respectively.

Of the 32 classes (i.e. terminal nodes) only two encompassed an area greater than 5% of the watershed. The terminal node with a persistence value of 4.5 covered 11% of the watershed – restricted to above-timberline areas in the west. As an example application of these results for observation network design the ten most spatially abundant classes were identified. The percentage of watershed area values are not significantly correlated with any of the independent variables and hence substantial variability in physiographics would be represented by an observation network located within each of these areas. The Lily Pond (4.1%), Middle Creek (6.4%), and Slumgullion (4.0%) SNOTEL sites were located within these 10 priority classes. Upper San Juan was located in a class that encompassed 3.5% of the watershed area with all other SNOTEL sites located in classes covering less than 2% of the watershed area. The Beartown SNOTEL site, not considered in this research, was located within a class with an areal extent less than 2% of the watershed area.

The ratio between the areal extent of a given terrain class and the deviance of snow cover persistence within the terrain class (i.e. extent / deviance ratio) ranged from 3.6×10^{-4} to 6.1×10^{-4} in the 3rd level of the regression tree (Figure 10). The greatest extent / deviance ratio (Figure 10) corresponded to the terminal node with a persistence

class covering 11% of the watershed. This terrain class exhibits a low amount of within-class deviance despite the large area it encompasses. Depending on the size of the desired network, the regression tree models and resultant extent / deviance ratios can be used to assess the degree to which those observations represent the surrounding terrain.

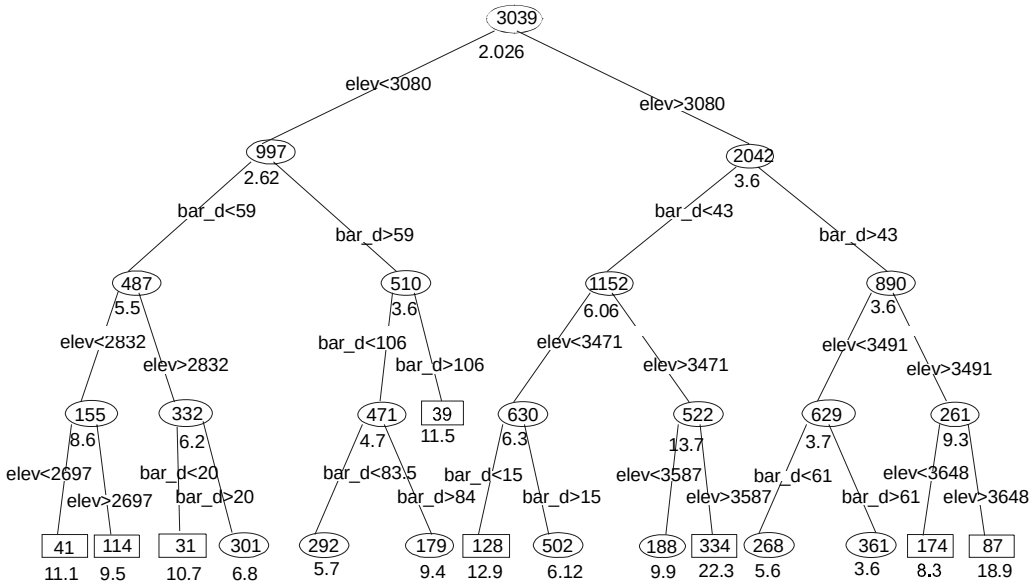

Figure 10. Top 5 levels of the regression tree shown in figure 12 with node values equal to the number of 1-km pixels represented by a given node. The value beneath each node is the ratio of the spatial extent of the given class (node) and the deviance of snow cover persistence with the respective node. Note: extent / deviance ratios are unitless and are shown as ratio x 10^{-4}.

DISCUSSION

This research has used remotely sensed data to estimate the variability in snow cover persistence – an indicator of both snow accumulation and snowmelt processes. Complimentary efforts aimed at estimating large scale SWE variability using remote sensing (Chang, et al., 1991; Chang and Rango, 2000; Foster, et al., 1991) and modeling (Carroll, et al., 2001; Martinec, 1991; Rango, 1988; Rango and Itten, 1976; Rango and Martinec, 1982; Shafer, et al., 1979) will benefit from the results presented here in that these works rely on ground observations to estimate model / algorithm performance. Using independent variables and binary classification models we have identified the types of snow cover environments currently represented by the SNOTEL network; e.g. the environments in which uncertainty in modeled and remotely sensed SWE estimates can be identified. Equally important, we have identified the snow cover environments not represented by SNOTEL observations; e.g. those where uncertainty in SWE estimates can't be obtained. Further, these areas need to be instrumented as part of observation networks that are tailored to spatial applications. To that end, we have outlined a statistically unbiased technique for locating potential future observations. We do not assert that these results are transferable to other locations nor do we suggest that SNOTEL stations be moved. However, the techniques for locating future observations and for assessing the relationship between snowpack processes and physiographics are widely transferable given the global coverage of the satellites used in this research and the global availability of topographic data at 1-km resolution.

Scaling of measurements and parameterizations of hydrologic state variables and processes is an increasingly daunting problem, as technological advances in observation capabilities at various scales emerge. A concept for addressing these scaling issues was posed by Wood et al. (1990; 1988) in which they assert the need to identify a representative elementary area (REA) at which a model element (or sub-catchment) contains a sufficient sample of the continuum of hillslope and soil characteristics such that the pattern of those characteristics can be ignored. Estimating this continuum requires information at the next smallest scale (Beven, 1995). Given that passive

microwave SWE data are not available at scales less than (25 km^2), we use a compromise to SWE in which the continuum of snowpack processes are estimated at the scale of optical remote sensing data products (i.e. 1-km).

The accuracy of modeled and remotely sensed estimates of SWE varies non-linearly in different physiographic conditions. Therefore, future networks must also be located in areas that span the continuum of large-scale variability. We have shown that SNOTEL stations are not located in the high-elevation, alpine areas closest to the western barrier or in areas with intermittent snow cover toward the eastern side of the watershed. Considerable effort needs to be placed on including these types of areas in future networks, particularly those areas with lower SWE accumulation, as snow distribution behaves in increasingly non-linear ways as snow accumulation decreases (Blöschl, 1999).

We have presented the first use of binary regression tree models to study large-scale (e.g. > 1000 km^2) patterns in snowpack processes. Previous applications of regression tree models at these scales have focused on estimating fractional snow covered area at a snap-shot in time (Rosenthal, 1996; Rosenthal and Dozier, 1996). Process level understanding of physiographic controls on snow accumulation have been obtained using regression tree models at scales less than 100 km^2 (Balk and Elder, 2000; Elder, et al., 1995; Erxleben, et al., 2002; Molotch, et al., 2005; Winstral, et al., 2002). The results presented here are complimentary to these previous works in that the regional-scale controls on snowpack processes were assessed, leaving the task of identifying hillslope-scale controls on snowpack processes to the aforementioned works.

Although snow cover persistence is highly correlated with elevation (R^2 = 0.61) we have shown that western barrier distance can further explain persistence patterns. Hence, hydrologic studies that estimate runoff and snow water equivalent based on rates of snow cover depletion within watershed clusters (Lee, et al., in press; Martinec, 1991; Rango, 1988; Rango and Martinec, 1982) may benefit from more complex basin clustering schemes such as presented here. Furthermore, observations placed in the locations suggested under this research would dramatically expand upon the narrow range of conditions in which these aforementioned works were evaluated (Lee, et al., in press).

SNOTEL are located in areas with persistent snow cover relative to the average persistence across the watershed, however, we have shown that stations are only representative of a subset of conditions where persistence is greatest; high elevation areas closest to the western barrier are not currently represented despite the large spatial extent and low within-class deviance of these areas (Figure 10).

Areas with lower snow cover persistence were also not represented by SNOTEL. Observations of SWE in these areas would have considerable utility in a variety of spatial hydrologic applications. Snow cover depletion patterns in these areas correlate strongly with runoff from 1 April to 15 May (Lee, et al., in press) – yet model performance on the basis of snowpack observations in these areas remains unidentified. Works that explicitly represent land-surface / atmosphere energy exchange and the distribution of snow water equivalent within high resolution (e.g. 30-m) grid-elements (Molotch, et al., 2004a) would benefit from observations of SWE in areas of lower snow cover persistence to evaluate grid-element specific model performance in these un-sampled areas. Similar works at course resolution (e.g. 2.8˚) (Dickinson, 1988; Jin, et al., 1999; Yang, et al., 1999) require observations across a range of conditions – including areas of intermittent snow cover – to obtain average estimates of SWE across the model grid-element scale.

CONCLUSIONS

SNOTEL sites in and around the Rio Grande headwaters basin are not located in areas that are representative of the physiographic conditions of the watershed. Rather they are located at the middle elevations, in densely forested areas, and close to the western barrier. Snow cover persistence at SNOTEL stations ranged from 3.9 to 4.4 with an average 12% greater than the mean persistence of the watershed. Therefore SNOTEL are not located in areas that capture the variability in snowpack processes across the watershed. Using elevation, western barrier distance, and vegetation density a 32-node regression tree model explained 75% of the variability in snow-cover persistence with persistence increasing with elevation and decreasing with distance to the western barrier. We have presented an example observation network design in which we identified the top ten spatially abundant terrain classes as optimal for instrumentation. The percent of watershed area represented by each of these classes were not significantly correlated with any of the independent variables and therefore substantial variability in physiographics would be

captured by the proposed network. Currently, the terrain classes encompassing the Lily Pond, Middle Creek, and Slumgullion SNOTEL sites were within the identified optimal areas, representing 4.1, 6.4, and 4.0% of the watershed area, respectively. SNOTEL stations do not exist in the most spatially extensive (11% of the watershed) terrain class located in the upper elevations above timberline. The results and techniques presented here will be useful for spatially distributed hydrologic analyses in that we have identified the physiographic conditions currently represented by SNOTEL stations. Further, we have outlined a statistically unbiased approach for designing future observation networks based on variability in physiographics and snowpack processes.

ACKNOWLEDGEMENTS

S. Fassnacht, R. Brice, R. Davis, W. Rosenthal, C. McKenzie, S. Leake, M. Gillespie, T. Pagano and others are all thanked for technical support. This research was supported by a visiting fellowship at the Cooperative Institute for Research in Environmental Sciences (CIRES), University of Colorado at Boulder, National Oceanic and Atmospheric Administration (NOAA). Additional support was provided by SAHRA (Sustainability of semi-Arid Hydrology and Riparian Areas) under the STC Program of the National Science Foundation, Agreement No. EAR-9876800 and by the Climate Assessment for the Southwest (CLIMAS), Institute for the Study of Planet Earth.

REFERENCES

Anderton, S.P., S.M. White, and B. Alvera. 2004. Evaluation of spatial variability in snow water equivalent for a high-mountain catchment. Hydrological Processes 18: 435-453.

Bales, R.C., R. Brice, B. Imam, and D. Lampkin. 2003. Seasonal and Interannual Variability in Colorado River and Rio Grande snowcover patterns: 1995-2002. Eos Trans. AGU, Fall Meeting Supplement, *84*.

Balk, B., and K. Elder. 2000. Combining binary decision tree and geostatistical methods to estimate snow distribution in a mountain watershed. Water Resources Research 36: 13-26.

Beven, K. 1995. Linking parameters across scales: subgrid parameterizations and scale dependent hydrological models. Hydrological Processes 9: 507-525.

Blöschl, G. 1999. Scaling issues in snow hydrology, Hydrological Processes 13: 2149-2175.

Breiman, L., J. Friedman, R. Olshen, and C. Stone. 1984. Classification and Regression Trees, Wadsworth and Brooks, Pacific Grove, CA., 358 p.

Carroll, T.R., D.W. Cline, G. Fall, A. Nilsson, L. Li, and A. Rost. 2001. NOHRSC operations and the simulation of snow cover properties for the coterminous U.S., Proceedings of the 69th Western Snow Conference, pp. 1-14.

Chambers, J., and T. Hastie (1993), Statistical Models in S, 608 pp., Chapman and Hall, London, UK.

Chang, A., J. Foster, and A. Rango. 1991. Utilization of surface cover composition to improve the microwave determination of snow water equivalent in a mountain basin, International Journal of Remote Sensing 12: 2311-2319.

Chang, A.T.C., and A. Rango. 2000. Algorithm theoretical basis document for the AMSR-E snow water equivalent algorithm, Version 3.1., NASA Goddard Space Flight Center, Greenbelt, MD, USA.

Cline, D.W., and T.R. Carroll. 1999. Inference of snow cover beneath obscuring clouds using optical remote sensing and a distributed snow energy and mass balance model, Journal of Geophysical Research 104: 19631-19644.

Davis, R.E., J.P. Hardy, W. Ni, C.E. Woodcock, J.C. McKenzie, R. Jordan, and X. Li. 1997. Variation of snow cover ablation in the boreal forest: A sensitivity study on the effects of conifer canopy, Journal of Geophysical Research 102: 29389-29395.

Dickinson, R.E. 1988. The force-resore model for surface temperatures and its generalization, Journal of Climate 1: 1086-1097.

Dozier, J. 1980. A clear-sky spectral solar radiation model for snow-covered mountainous terrain, Water Resources Research 16: 709-718.

Elder, K. 1995. Snow distribution in alpine watersheds, Dissertation thesis, University of California, Santa Barbara. 309 p.

Elder, K., J. Michaelsen, and J. Dozier. 1995. Small basin modeling of snow water equivalence using binary regression tree methods, paper presented at Biogeochemistry of Seasonally Snow-Covered Catchments. IAHS Publication No. 228. IAHS: Wallingford, Boulder, Colorado, pp. 129-139.

Elder, K., W. Rosenthal, and R. Davis. 1998. Estimating the spatial distribution of snow water equivalence in a montane watershed, Hydrological Processes 12: 1793-1808.

Erxleben, J., K. Elder, and R. Davis. 2002. Comparison of spatial interpolation methods for estimating snow distribution in the Colorado Rocky Mountains, Hydrological Processes 16: 3627-3649.

Fassnacht, S.R., K.A. Dressler, and R.C. Bales. 2001. Physiographic parameters as indicators of snowpack state for the Colorado River Basin, Proceedings of the 58th Eastern Snow Conference, pp. 45-48.

Fassnacht, S.R., K.D. Dressler, and R.C. Bales. 2003. Snow water equivalent interpolation for the Colorado River Basin from snow telemetry (SNOTEL) data, Water Resources Research, 39, 10.1029/2002WR001512.

Foster, J., A. Chang, D. Hall, and A. Rango. 1991. Derivation of snow water equivalent in boreal forests using microwave radiometry, Arctic 44: 147-152.

Gray, D., and D. Male. 1981. Handbook of snow, Pergamon Press, Toronto, Canada. 776 p.

Jin, J., X. Gao, S. Sorooshian, Z.L. Yang, R.C. Bales, R.E. Dickinson, S.F. Sun, and G.X. Wu. 1999. One-dimensional snow water and energy balance model for vegetated surfaces, Hydrological Processes 13: 2467-2482.

Klein, A., and J. Stroeve. 2002. Development and validation of a snow albedo algorithm for the MODIS instrument, Annals of Glaciology 34: 45-52.

Lee, S., A.G. Klein, and T.M. Over (in press), A comparison of MODIS and NOHRSC snow-cover products for simulating streamflow using the snowmelt runoff model, Hydrological Processes, doi: 10.1002/hyp.5810.

Martinec, J. 1991. Areal modelling of snow water equivalent based on remote sensing techniques, Snow Hydrology and Forests in High Alpine Areas: Proceedings of the Vienna Symposium, IAHS Publication No. 205, pp. 121 - 129.

Molotch, N., P., T.H. Painter, R.C. Bales, and J. Dozier. 2004a. Incorporating remotely sensed snow albedo into a spatially distributed snowmelt model, Geophysical Research Letters 31: 10.1029/2003GL019063.

Molotch, N.P., M.T. Colee, R.C. Bales, and J. Dozier. 2005. Estimating the spatial distribution of snow water equivalent in an alpine basin using binary regression tree models: the impact of digital elevation data and independent variable selection, Hydrological Processes 19: 10.1002/hyp.5586.

Molotch, N. P., S. R. Fassnacht, R. C. Bales, and S. R. Helfrich. 2004b. Estimating the distribution of snow water equivalent and snow extent beneath cloud-cover in the Salt-Verde River basin, Arizona, Hydrological Processes, 18, 10.1002/hyp.1408.

National Research Council - Cline D., R.E. Davis, and S. Yueh. 2005. Cold-land processes pathfinder mission concept, Space Studies Board National Academy of Sciences.

Painter, T.H., J. Dozier, D.A. Roberts, R.E. Davis, and R.O. Green. 2003. Retrieval of subpixel snow-covered area and grain size from imaging spectrometer data, Remote Sensing of Environment 85: 64-77.

Rango, A. 1988. Progress in developing an operational snowmelt-runoff forecast model with remote sensing input, Nordic Hydrology 19: 65-75.

Rango, A., and K. Itten. 1976. Satellite potentials in snowcover monitoring and runoff prediction, Nordic Hydrology 7: 209-230.

Rango, A., and J. Martinec. 1982. Snow accumulation derived from modified depletion curves of snow coverage, Hydrological Aspects of Alpine and High Mountain Areas (Proceedings of the Exeter Symposium), IAHS publ. No. 138, 83-89.

Rosenthal, W. 1996. Automated snow mapping at subpixel resolution from NOAA-AVHRR data, U.S. Army Cold Regions Research and Engineering Laboratory, Hanover, N.H.

Rosenthal, W., and J. Dozier. 1996. Automated mapping of montane snow cover at subpixel resolution from the Landsat Thematic Mapper, Water Resources Research 32: 115-130.

Shafer, B.A., C.F. Leaf, and J.K. Marron. 1979. Landsat derived snow cover as an input variable for snow melt runoff forecasting in South Central Colorado, in Satellite Hydrology, edited by M. Deutsch, et al., American Water Resources Association, Minneapolis, Minnesota, pp. 218-224.

Sicart, J.E., J.W. Pomeroy, R.E. Essery, J. Hardy, T. Link, and D. Marks. 2004. A sensitivity study of daytime net radiation during snowmelt to forest canopy and atmospheric conditions, Journal of Hydrometeorology 5: 774-784.

Simpson, J.J., J.R. Stitt, and M. Sienko. 1998. Improved estimates of the areal extent of snow cover from AVHRR data, Journal of Hydrology 204: 1-23.

Solomon, S.I., J.P. Denouvilliez, E.J. Chart, J.A. Wooley, and C. Cadou. 1968. The use of a square grid system for computer estimation of precipitation, temperature, and runoff, Water Resources Research 4: 919-929.

U.S. Soil Conservation Service. 1972. Snow survey and water supply forecasting. Section 22, SCS Nat. Eng. Handbook, U.S. Department of Agriculture, Washington, D.C.

Winstral, A., K. Elder, and R. Davis. 2002. Spatial snow modeling of wind-redistributed snow using terrain-based parameters, Journal of Hydrometeorology 3: 524-538.

Wood, E.F., M. Sivapalan, and K.J. Beven. 1990. Similarity and scale in catchment storm response, Reviews of Geophysics 28: 1-18.

Wood, E.F., M. Sivapalan, K.J. Beven, and L. Band. 1988. Effects of spatial variability and scale with implications to hydrological modelling, Journal of Hydrology 102: 29-47.

Yang, Z.L., R.E. Dickinson, A.N. Hahmann, G.Y. Niu, M. Shaikh, X. Gao, R.C. Bales, S. Sorooshian, and J. Jin. 1999. Simulation of snow mass and extent in general circulation models, Hydrological Processes 13: 2097-2113.